arXiv:2006.06201v1 [cs.CV] 11 Jun 2020

Fall Detector Adapted to Nursing Home Needs through an Optical-Flow based CNN

Alexy CARLIER[1*], Paul PEYRAMAURE[1*], Ketty FAVRE[2] and Muriel PRESSIGOUT[1]

***Abstract*— Fall detection in specialized homes for the elderly is challenging. Vision-based fall detection solutions have a significant advantage over sensor-based ones as they do not instrument the resident who can suffer from mental diseases. This work is part of a project intended to deploy fall detection solutions in nursing homes. The proposed solution, based on Deep Learning, is built on a Convolutional Neural Network (CNN) trained to maximize a sensitivity-based metric. This work presents the requirements from the medical side and how it impacts the tuning of a CNN. Results highlight the importance of the temporal aspect of a fall. Therefore, a custom metric adapted to this use case and an implementation of a decision-making process are proposed in order to best meet the medical teams requirements.**

Clinical relevance **This work presents a fall detection solution enabled to detect 86.2% of falls while producing only 11.6% of false alarms in average on the considered databases.**

I. INTRODUCTION

In specialized homes for the elderly, fall is the leading cause of death due to trauma as a resident falls 1.7 times a year in average in France [1]. Some of them being more or less prone to falls, medical teams may discover a person who has fallen to the ground only after several hours [2]. In this context, a fall detector must detect falls while avoiding false alarms unnecessarily disturbing to the medical staff, which can not afford too frequent and intuitive interruptions. According to a study [3] conducted with specialized medical teams, residents and families in three different nursing homes, the solution must:

- detect as many falls as possible;
- give no false alarms;
- not be an extra equipment to be worn by the resident;
- be re-configurable and adaptable to different residents.

Fall detection solutions are divided into two types of approaches: sensor-based and vision-based. This work focuses on vision-based solutions since wearable sensor-based ones do not meet medical staff requirements. Indeed, they are not adequate when dealing with people suffering from mental diseases which is more frequent with older people. Moreover, even if a camera can cause privacy issues, the study shows that majority of medical teams, residents and families approve its use for residents safety and independence.

In general, a fall leads to a change of the human body velocity and position. Thus, in image-based techniques, features such as 2D human body pose estimation [4], movement vectors or person silhouettes using background subtraction algorithms [5] are extracted from images. These features, enabling to locate the person and know its spatial body orientation, are usually fed to a classifier such as Gaussian Mixture Model (GMM) [6] or Support Vector Machine (SVM) [7] [8]. The difficulty to characterize falls led the community to consider its temporal aspect. The use of Long Short-Term Memory (LSTM) [9] networks enables advances in vision-based fall detection. Another approach is to feed several RGB images directly to a 3D Convolutional Neural Network (CNN) [10] [11] to exploit their temporal aspect.

Due to disabilities and/or old age, elderly falls can be characterized by different types and velocities of movement: hard falls (from standing position) and soft falls (from another starting point). They are therefore very difficult to model. Thus, a solution based on a neural network that takes into account human body motion changes seems to be adapted to this problem. The presented solution is optical-flow based and uses a CNN originally trained to maximize a sensitivity metric [12]. We propose a different training approach using realistic metrics adapted to the application as well as a decision-making process adjustment which minimizes the number of false alarms and ensures a sufficient correct detection rate according to medical staff requirements.

II. METHODOLOGY

A. Solution overview

The general solution presented in Fig. 1 is made of three stages. The first step takes as input two consecutive RGB images from a camera to generate a pair of optical flow images using the dense optical-flow TV-L1 algorithm [13]. The second step of the solution is a custom VGG-16 CNN designed as in [14] and pre-trained as in [12]. It takes as input a stack S of $L = 10$ consecutive pairs of optical flow images and infers a fall prediction. Finally, a custom temporal filter and a prediction threshold are applied to the CNN output in order to exploit the fall temporal aspect. In this way, a single or consecutive stacks S, labeled as *Fall* at the temporal filter output, raise a fall alarm to the medical staff.

B. Databases and training procedure

Three labeled fall video databases (URFD [15], FDD [16], Multicam [17]) are used for the training and test processes. They are composed of videos containing a fall action or not. Those which contain daily-life actions are annotated as *non-fall*. Fall videos are split into three parts: the *pre-fall* which is the action time before the fall, the *fall* action, and the *post-fall* which often corresponds to a person lying

[1]Univ Rennes, INSA Rennes, CNRS, IETR - UMR 6164, Rennes, France.
[2]Univ Rennes, CNRS, IETR - UMR 6164, Rennes, France.
*Both authors contributed equally to this work.

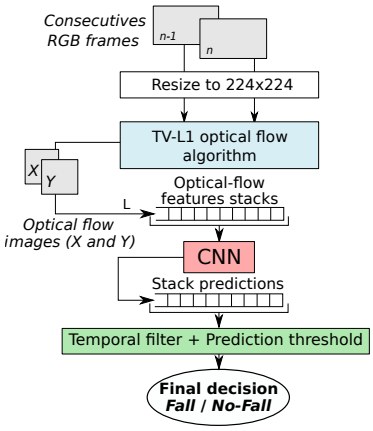


Fig. 1. Solution overview from the input (RGB frames) to the output (final decision *Fall* / *No-Fall*)

on the ground. The classifier of the CNN has two output classes: *Fall* and *No-Fall*. *Fall* class contains *fall* actions and *No-Fall* class takes into account *pre-fall*, *post-fall* and *non-fall* video sequences. Fall action databases usually contain more daily-life actions than falls. In order to fine-tune the classifier, which is composed by two last Fully-Connected (FC) layers of the CNN, and overcome unbalanced data, a weighted binary cross-entropy loss function (1) is adopted as proposed in [12]. In that equation, p is the prediction of the network, t is the ground-truth, the class weight w_0 is associated to *Fall* class and w_1 to *No-Fall* class.

$$loss(p,t) = -(w_1 \,.\, t \,.\, log(p) + w_0 \,.\, (1-t) \,.\, log(1-p)) \quad (1)$$

Leveraging on transfer-learning, it is possible to achieve fall detection while the amount of data is limited. All network layers except the last two FC layers are frozen. That two last FC are trained with fall databases using the 5-cross fold validation [18]. In order to have a training framework usable for any other database, our training approach differs from [12] on these points:

- During the 5-cross fold validation, each video sequence is entirely stored in a single fold. It avoids having similar stacks in the train set and in the test set. Moreover, the train set and the validation set are filled with different videos in order to avoid overfitting. Then for a given initial fall video sequence, the derived sequences *pre-fall*, *fall* and *post-fall* are in the same fold.
- At testing time, a *Transition* class is used in addition to *Fall* and *No-Fall* classes in order to bring realistic cases. This class contains frames at the transition between *pre-fall* and *fall* and the transition between *fall* and *post-fall* sequences. These particular testing frames are not used in [12] and [14].

In order to obtain the best training efficiency possible, a grid search methodology is used with the following hyper-parameter ranges:

- Learning rate λ: $\{10^{-2}, 10^{-3}, 10^{-4}, 10^{-5}, 10^{-6}\}$
- Batch size Bs: {128, 256, 512, 1024}
- Class weight w_0: {1, 2, 5, 10, 15, 20} and w_1: {1}
- Classifier activation function f_{act}: {ELU, ReLU}

Configurations are evaluated through specificity sp (2), sensitivity se (3) and precision p (4) where TP stands for True Positives, TN for True Negatives, FP for False Positives and FN for False Negatives. These metrics are computed over stack predictions and are used to choose the best hyper-parameters configuration.

$$sp = TN/(TN+FP) \quad (2)$$

$$se = TP/(TP+FN) \quad (3)$$

$$p = TP/(TP+FP) \quad (4)$$

In [12], authors focus on maximizing sensitivity which leads to a decrease of specificity and precision. In our case, according to medical staff requirements which are explained in section I, specificity and precision are favored and it must be a trade-off with the sensitivity.

C. Alarm precision oriented fall evaluation

It is difficult to determine the exact beginning and end of a fall which makes it a complex event to characterize. Furthermore, the duration of a fall must be taken into account when evaluating the predictions. As presented in section II-A, the network makes a prediction with L consecutive optical flow images. In the considered databases, the average fall duration is 1.11 seconds as seen in Table I. This means that a fall prediction is made during 1/3 of the average fall duration considering a 30 FPS recording. The addition of a temporal filter, as defined below, reinforces the time aspect of a fall and aggregates safe signals while reducing false alarms.

TABLE I
DATABASES PROPERTIES

Database	Frame rate (FPS)	Avg. fall duration (frames - seconds)	Number of falls
URFD	30	30 - 1.00	30
FDD	25	24 - 0.96	99
Multicam	30	41 - 1.36	200
Avg.	28	32 - 1.11	-

In the temporal analysis step, predictions are considered no longer as stacks but as consecutive identical stack prediction types. They are labeled either as TP_a for a true fall alarm, as FP_a for a false fall alarm, or as FN_a for a miss-detected fall. The implemented convolution filter is modeled by a gate function. It is defined by its width W (in frames or seconds) conjointly tuned with the prediction threshold T_{pred} of the filter. Below T_{pred}, a prediction is labeled as fall. These parameters are adjusted with the aim of minimizing the number of false alarms without missing falls. To measure this capability, F_β (7) is a function of the alarm precision p_a (5) and the alarm sensitivity se_a (6) in the same spirit as in [19]. When $0 < \beta < 1$, F_β metric weighs sensitivity less than precision by emphasizing more on false alarms and inversely when $\beta > 1$. This metric enables a realistic fall detector evaluation with respect to the medical requirements.

$$p_a = TP_a/(TP_a + FP_a) \quad (5)$$

$$se_a = TP_a/(TP_a + FN_a) \quad (6)$$

$$F_\beta = (1+\beta^2) \,.\, \frac{p_a \,.\, se_a}{(\beta^2 \,.\, p_a) + se_a} \quad (7)$$

III. EXPERIMENTS

A. Hyper-parameters choice

Hyper-parameters of the CNN training are adjusted regarding the previously exposed specifications, namely a trade-off between high specificity and sufficient sensitivity.

The first hyper-parameter to be tuned is the **learning rate** λ. From the studied values, 10^{-2} is too high and causes the model to diverge. On the other hand, the model converges too slowly for a learning rate lower than 10^{-4}.

Concerning the **batch size** Bs, the choice made in [12] (i.e. 1024) may not lead to a well converged model as it was too high. From our experiments, a smaller batch size (of 128 or 256) leads to a better specificity. It deteriorates the sensitivity se due to an increase of FN but leads to a small impact on the alarm sensitivity se_a.

The **activation function** ELU leads to a better sensitivity than the ReLU activation function that gives a better specificity. ReLUs are therefore chosen for our use case.

Finally, a Receiver Operating Characteristic (ROC) analysis is made on the **class weight** w_0 (w_1 is arbitrarily set to 1) to put emphasis on *Fall* class and select the configuration giving the best specificity. In practice, w_0 higher than 5 implies instabilities in results both with balanced and unbalanced amounts of data in each class. w_0 set to 2, as in [12], slightly increases the specificity and avoids overfitting on the $Fall$ class. Best configurations giving a well-trained model with an acceptable specificity are summarized in Table II.

TABLE II

BEST TRAINING CONFIGURATIONS AND ASSOCIATED RESULTS (IN %)

ID	λ	w_0	Bs	f_{act}	URFD		FDD		Multicam	
					se	*sp*	*se*	*sp*	*se*	*sp*
1	10^{-3}	2	128	ReLU	95.5	93.2	94.7	97.5	**56.5**	**99.4**
2	10^{-3}	2	256	ReLU	**89.5**	**94.1**	**93.5**	**97.6**	59.4	99.0
3	10^{-4}	2	128	ReLU	93.5	88.7	95.2	97.5	68.2	96.0
4	10^{-4}	2	256	ReLU	95.5	89.2	96.0	96.9	71.4	93.7

B. Temporal Analysis

In order to improve model performances, prediction results are analyzed during training following their temporal aspect using metrics presented in section II-C. An analysis of the number of frames between FP_a and *Fall* labels, defined as offset in Fig. 2, allows to better characterize false alarms.

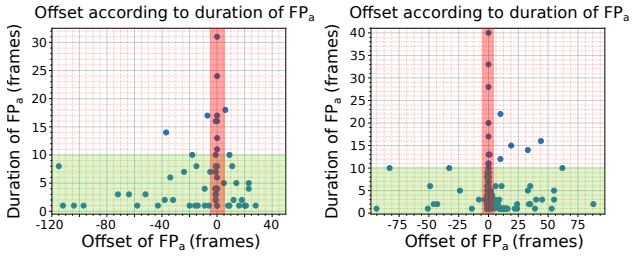


Fig. 2. Offset to the *Fall* class according to the duration of FP_a. The horizontal zone (in green) includes FP_a duration shorter than 10 frames. The vertical zone (in red) includes FP_a offset smaller than 5 frames. URFD on the left and FDD on the right.

In the three databases, 39% of FP_a are very close in time to the actual fall with an offset smaller than 5 frames. These predictions are labeled as false according to the ground-truth but are ambiguous. Indeed, they could be considered as the beginning or the end of the related fall from a human perception. Secondly, 86% of FP_a are shorter than 10 frames and will be removed by the temporal filter application.

Table III shows the evaluation results of the CNN output predictions, with $T_{pred} = 0.5$, using the theoretical precision metric p computed with stack predictions, the alarm precision p_a and the alarm sensitivity se_a. Concerning all databases, p_a is significantly lower than p which is expected as the temporal property is not taken into account yet.

TABLE III

TEMPORAL EVALUATION OF THE CNN OUTPUT PREDICTIONS WITH $T_{pred} = 0.5$ AND TRAINING CONFIGURATION ID 2 (IN %)

Database	p	p_a	se_a
URFD	47.0	27.0	100
FDD	59.1	54.7	98.9
Multicam	63.6	25.5	89.0
Avg.	56.6	35.7	96.0

C. Filter size and prediction threshold adjustments

An empirical study, illustrated in Fig. 3, is made in order to propose the best association between the temporal filter size W and the prediction threshold T_{pred}. Our use case suggests to maximize the alarm precision p_a while stabilizing the alarm sensitivity se_a on the three considered databases.

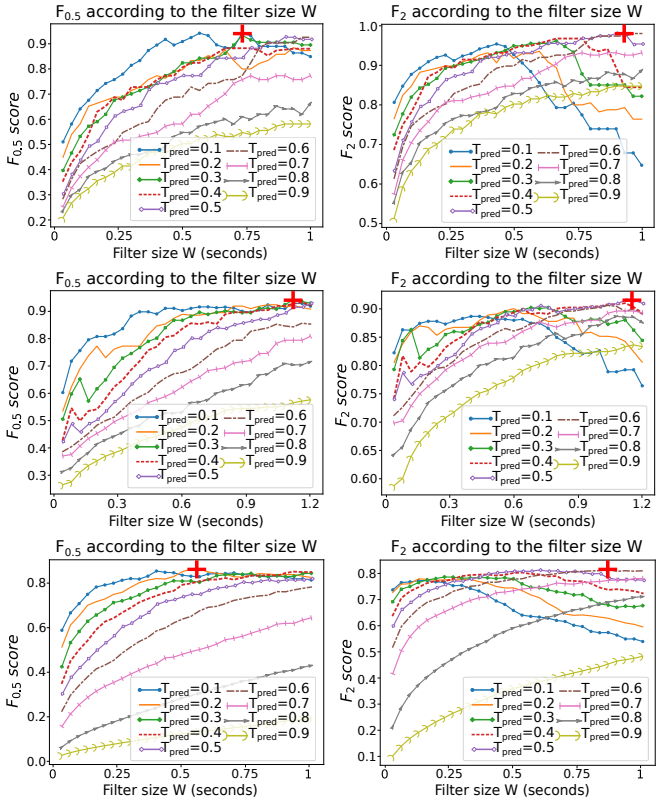


Fig. 3. $F_{0.5}$ (at left) and F_2 (at right) according to filter size W in seconds. Each graph plots curves for a T_{pred} ranging from 0.1 to 0.9. Red crosses annotate configurations reaching the maximal F_β. From top to bottom, graphs correspond to the three databases: URFD, FDD and Multicam.

$F_{0.5}$ and F_2 decrease as T_{pred} is getting larger due to the rise of undetected falls. From a certain W value, F_2 is reduced due to the same reason. For Multicam database, the number of undetected fall sequences is important and comes from the fact that it is a complex database with inaccuracies in labeling. The sequences are also much longer and more complex in terms of action. The objective is to drastically decrease the number of false alarms while limiting the number of undetected falls. In our case, p_a is fixed to be more than 80% and se_a must not vary more than 10% from Table III. The optimal (W, T_{pred}) pair is found by averaging (W, T_{pred}) pairs that maximize F_β for each database.

In the end, $W = 0.87$ sec and $T_{pred} = 0.4$ are found to be the best combination and lead to the results in Table IV. Compared to Table III, the alarm precision p_a increases drastically from 35.7% to 88.4% with the optimal (W, T_{pred}). On the other hand, the alarm sensitivity se_a decreases from 96.0% to 86.2% per database in average. This means that the solution detects 86.2% of falls while 88.4% of the raised alarms are real falls. Considering the best camera (on which the fall is best visible) on Multicam database, the results of our solution are 7% higher in terms of alarm precision and 4% in terms of alarm sensitivity than in [19].

TABLE IV
FINAL RESULTS (IN %) WITH THE TUNED DECISION PROCESS: W = 0.87 SEC AND T_{pred} = 0.4

Database	$F_{0.5}$	F_2	p_a	se_a	TP_a	FP_a	FN_a
URFD	87.4	94.2	85.3	96.7	29	5	1
FDD	92.4	91.3	92.8	90.9	90	7	9
Multicam	83.3	73.7	87.1	71.0	142	21	58
Avg.	87.7	86.4	88.4	86.2	-	-	-
Multicam[1]	**89.1**	**91.3**	**88.5**	**92.0**	**23**	**3**	**2**
Multicam[2]	82.7	86.6	81.5	88.0	22	5	3

[1] Our method on the best camera
[2] Method of [19] on the best camera

IV. CONCLUSION

In this study, we brought a new perspective on fall detection solutions focused on the application in nursing homes. This vision has led to a new CNN training strategy driven by a realistic alarm rate metric and a decision-making process that fits medical staff expectations. The presented solution has proven to detect 86.2% of falls while producing only 11.6% of false alarms in average on the considered databases. The analysis of false alarms has shown that in most cases they occur when the person sits down heavily, stands up after a fall or gets down to pick up something on the ground.

Our future works on that topic include the implementation of a spatial filter such as semantic background segmentation and an increase of the number and diversity of data in order to enhance the results. The system has been tuned and tested on fall videos simulated by performers, hence the next step would be to conduct a clinical study. Another opportunity would be to leverage on multiple cameras data fusion as in Multicam database within results analysis shows that a fall is always detected by at least one camera over all.

ACKNOWLEDGMENT

This work was founded by the European Union, the Britanny region in France and the French city of Rennes through the AAP FEDER - SilverConnect project.

The authors thank the "Pole Saint-Helier" which conducted the study in three different specialized homes for the elderly in the metropolitan area of Rennes, France.

REFERENCES

[1] Juliette Podvin-Deleplanque, Daniel Dreuil, Dominique Huvent, and Franois Puisieux, "Fall Prevention in Nursing Homes," *La Revue de Griatrie*, p. 8, 2015, (Prvention des chutes en EHPAD).

[2] Jane Fleming and Carol Brayne, "Inability to get up after falling, subsequent time on floor, and summoning help: prospective cohort study in people over 90," *BMJ*, vol. 337, pp. a2227, Nov. 2008.

[3] Bastien Fraudet, Emilie Leblong, Marie Dandois, Estelle Ceze, and Berenice Rocabado, "SILVER CONNECT project: Requirements gathering and acceptability," Technical Report, Living lab ISAR, Ple Saint Hlier, May 2020.

[4] Wen-Nung Lie, Anh Tu Le, and Guan-Han Lin, "Human fall-down event detection based on 2D skeletons and deep learning approach," in *2018 International Workshop on Advanced Image Technology (IWAIT)*, Chiang Mai, Jan. 2018, pp. 1–4, IEEE.

[5] Glen Debard, Greet Baldewijns, Toon Goedeme, Tinne Tuytelaars, and Bart Vanrumste, "Camera-based fall detection using a particle filter," in *2015 37th Annual International Conference of the IEEE Engineering in Medicine and Biology Society (EMBC)*, Milan, Aug. 2015, pp. 6947–6950, IEEE.

[6] Caroline Rougier, Jean Meunier, Alain St-Arnaud, and Jacqueline Rousseau, "Robust Video Surveillance for Fall Detection Based on Human Shape Deformation," *Circuits and Systems for Video Technology, IEEE Transactions on*, vol. 21, pp. 611–622, June 2011.

[7] Imen Charfi, Johel Miteran, Julien Dubois, Mohamed Atri, and Rached Tourki, "Definition And Performance Evaluation Of A Robust SVM Based Fall Detection Solution," Nov. 2012.

[8] Nabil Zerrouki, Fouzi Harrou, Amrane Houacine, and Ying Sun, "Fall detection using supervised machine learning algorithms: A comparative study," Nov. 2016, pp. 665–670.

[9] Mirto Musci, Daniele De Martini, Nicola Blago, Tullio Facchinetti, and Marco Piastra, "Online Fall Detection using Recurrent Neural Networks," Apr. 2018.

[10] Shengchao Li, Hao Xiong, and Xiumin Diao, "Pre-Impact Fall Detection Using 3D Convolutional Neural Network," in *2019 IEEE 16th International Conference on Rehabilitation Robotics (ICORR)*, June 2019, pp. 1173–1178.

[11] Markus D. Solbach and John K. Tsotsos, "Vision-Based Fallen Person Detection for the Elderly," in *2017 IEEE International Conference on Computer Vision Workshops (ICCVW)*, Oct. 2017, pp. 1433–1442.

[12] Adrian Nunez-Marcos, Gorka Azkune, and Ignacio Arganda-Carreras, "Vision-Based Fall Detection with Convolutional Neural Networks," *Wireless Communications and Mobile Computing*, vol. 2017, 2017.

[13] Javier Sanchez, Enric Meinhardt-Llopis, and Gabriele Facciolo, "TV-L1 optical flow estimation," *Image Processing On Line*, vol. 3, pp. 137–150, July 2013.

[14] Limin Wang, Yuanjun Xiong, Zhe Wang, and Yu Qiao, "Towards Good Practices for Very Deep Two-Stream ConvNets," July 2015.

[15] Bogdan Kwolek and Michal Kepski, "Human fall detection on embedded platform using depth maps and wireless accelerometer," *Computer Methods and Programs in Biomedicine*, vol. 117, no. 3, pp. 489–501, Dec. 2014.

[16] "Fall detection Dataset - Le2i - Laboratoire Electronique, Informatique et Image," FDD dataset.

[17] Edouard Auvinet, Caroline Rougier, Jean Meunier, Alain St-Arnaud, and Jacqueline Rousseau, "Multiple cameras fall data set," p. 24, Multicam dataset.

[18] Payam Refaeilzadeh, Lei Tang, and Huan Liu, "Cross-Validation," *Encyclopedia of Database Systems*, Jan. 2009.

[19] Glen Debard, Marc Mertens, Mieke Deschodt, Ellen Vlaeyen, Els Devriendt, Eddy Dejaeger, Koen Milisen, Jos Tournoy, Tom Croonenborghs, Toon Goedem, Tinne Tuytelaars, and Bart Vanrumste, "Camera-based fall detection using real-world versus simulated data: How far are we from the solution?," *Journal of Ambient Intelligence and Smart Environments*, vol. 8, no. 2, pp. 149–168, Mar. 2016.